

Published in final edited form as:

*J Immunol.* 2006 April 1; 176(7): 4410–4418.

## Spatial and Temporal Profiles for Anti-Inflammatory Gene Expression in Leukocytes during a Resolving Model of Peritonitis<sup>1</sup>

Amilcar S. Damazo<sup>2,†</sup>, Simon Yona<sup>2,\*</sup>, Roderick J. Flower<sup>\*</sup>, Mauro Perretti<sup>3,\*</sup>, and Sonia M. Oliani<sup>3,†,‡</sup>

<sup>†</sup>William Harvey Research Institute, London, United Kingdom

<sup>†</sup>Post-Graduation in Morphology, Federal University of São Paulo, São Paulo, Brazil

<sup>‡</sup>Department of Biology, Instituto de Biociências, Letras e Ciências Exatas, São Paulo State University, São Paulo, Brazil

### Abstract

The recent appreciation of the role played by endogenous counterregulatory mechanisms in controlling the outcome of the host inflammatory response requires specific analysis of their spatial and temporal profiles. In this study, we have focused on the glucocorticoid-regulated anti-inflammatory mediator annexin 1. Induction of peritonitis in wild-type mice rapidly (4 h) produced the expected signs of inflammation, including marked activation of resident cells (e.g., mast cells), migration of blood-borne leukocytes, mirrored by blood neutrophilia. These changes subsided after 48–96 h. In annexin 1<sup>null</sup> mice, the peritonitis response was exaggerated (~40% at 4 h), with increased granulocyte migration and cytokine production. In blood leukocytes, annexin 1 gene expression was activated at 4, but not 24, h postzymosan, whereas protein levels were increased at both time points. Locally, endothelial and mast cell annexin 1 gene expression was not detectable in basal conditions, whereas it was switched on during the inflammatory response. The significance of annexin 1 system plasticity in the anti-inflammatory properties of dexamethasone was assessed. Clear induction of annexin 1 gene in response to dexamethasone treatment was evident in the circulating and migrated leukocytes, and in connective tissue mast cells; this was associated with the steroid failure to inhibit leukocyte trafficking, cytokine synthesis, and mast cell degranulation in the annexin 1<sup>null</sup> mouse. In conclusion, understanding how inflammation is brought under control will help clarify the complex interplay between pro- and anti-inflammatory pathways operating during the host response to injury and infection.

<sup>1</sup>This work was supported by the Fundação de Amparo a Pesquisa do Estado de São Paulo (FAPESP) and Conselho Nacional de Desenvolvimento Científico e Tecnológico (CNPq) Brazil; the Arthritis Research Campaign (ARC; Grant ID 15755) U.K.; and in part by William Harvey Research Foundation, London, U.K. M.P. is a Senior Fellow of the ARC; S.Y. was funded by a Ph.D. studentship of the Nuffield Foundation U.K. (Oliver Bird Fund; RHE/00057/G), whereas R.J.F. is a Principal Research Fellow of the Wellcome Trust U.K. A.S.D. is funded by a Ph.D. Studentship from FAPESP (02/09920-0) and a Ph.D. “Sandwich” Studentship from Coordenação de Aperfeiçoamento de Pessoal de Nível Superior (CAPES-BEX0223/03-4). S.M.O. is funded by FAPESP (03/11292-0) and CNPq (300943/1994-6).

<sup>3</sup>Address correspondence and reprint requests to Dr. Mauro Perretti, Centre for Biochemical Pharmacology, William Harvey Research Institute, Bart's and The London, Queen Mary School of Medicine and Dentistry, London EC1M 6BQ, U.K.; E-mail address: m.perretti@qmul.ac.uk or Dr. Sonia M. Oliani, Department of Biology, Instituto de Biociências, Letras e Ciências Exatas, São Paulo State University, São José do Rio Preto, São Paulo 15054-000, Brazil; E-mail address: smoliani@ibilce.unesp.br.

<sup>2</sup>A.S.D. and S.Y. contributed equally to this research.

The costs of publication of this article were defrayed in part by the payment of page charges. This article must therefore be hereby marked *advertisement* in accordance with 18 U.S.C. Section 1734 solely to indicate this fact.

#### Disclosures

The authors have no financial conflict of interest.

Understanding how the inflammatory response is controlled to prevent its overshooting and regulate its duration has been a recent task for those studying this crucial process of the host. Following infection or a xenobiotic insult, a coordinated response is mounted by the host characterized by several changes occurring within the microvessels of the affected organ (1, 2). One of the ensuing events is the trafficking of blood-borne leukocytes. This is regulated by several soluble or cell-anchored mediators, including adhesion molecules and leukocyte activators, which act in concert to induce and promote the time-dependent process of cell rolling, adhesion, and emigration (or diapedesis) (3, 4). The complex process of cell migration into inflamed tissues is finely regulated and controlled, to prevent its overactivity, hence the risk of tissue injury (5, 6). To this end, endogenous pathways operate in the host and act at different phases of the leukocyte extravasation process to counteract the action of proinflammatory mediators (7, 8). Few studies, though, have investigated when and where a given counterregulatory mediator, or its controlling gene, is activated during an ongoing inflammatory response.

Over the last decade, we and others have unraveled the anti-inflammatory properties of the glucocorticoid-regulated protein annexin 1 (AnxA1) (see Refs. 9 and 10 for recent reports). Distinguished from other annexins by its unique N-terminal region, AnxA1 is particularly abundant in neutrophils, up to 4% of the cytosolic proteins (11), and upon cell adhesion, it translocates onto the cell surface (12, 13), where it interacts with an anti-inflammatory receptor (14). Pharmacologically, human recombinant AnxA1 or peptides derived from the N-terminal region down-regulate neutrophil activation and trafficking (15-18).

The pathophysiological role of the endogenous protein can be now addressed because of the availability of null mice. These animals exhibit an exacerbation of acute and chronic experimental inflammatory responses (10, 19). Interestingly, partial resistance to the anti-inflammatory actions of dexamethasone (Dex)<sup>4</sup> was reported in these studies, confirming previous analyses conducted with immunoneutralization strategies (20, 21).

There is some evidence that once neutrophils migrate to inflammatory sites, large amounts of AnxA1 are synthesized and, in some cases, released (22-24); thus, besides its role within the microenvironment of the adherent neutrophil entering into diapedesis (12), exudate AnxA1 might have other roles including, for instance, the recently reported promotion of phagocytosis of apoptotic neutrophils by macrophages (25). However, the time course of expression and the major cellular sources for this important homeostatic protein are only a matter of speculation.

In an ultrastructural analysis of the rat-inflamed mesenteric microcirculation, we have reported that tissue-migrated neutrophils express higher AnxA1 levels, perhaps consequent to de novo synthesis, as determined by quantitative electron microscopy analysis and in situ hybridization (26). In this study, we have taken advantage of a reporter gene inserted into the construct used to generate the AnxA1<sup>null</sup> mice (19) to study gene expression and function of this anti-inflammatory protein in a resolving model of peritonitis (27, 28), performing a systematic analysis of its spatial and temporal distribution. In addition, the impact on this process on the anti-migratory effect of Dex was also evaluated.

---

<sup>4</sup>Abbreviations used in this paper: Dex, dexamethasone; WT, wild type; PMN, polymorphonuclear; X-Gal, 5-bromo-4-chloro-3-indolyl  $\beta$ -D-galactoside; M $\phi$ , macrophage; mono-M $\phi$ , monocyte-M $\phi$ .

## Materials and Methods

### Animals

Male wild-type (WT) littermate and *AnxA1*<sup>null</sup> mice (19) (20–25 g of body weight), maintained on a standard chow pellet diet with tap water ad libitum, were used for all experiments. Animals were housed at a density of five animals per cage in a room with controlled lighting (lights on from 8:00 a.m. to 8:00 p.m.) in which the temperature was maintained at 21–23°C. Animal work was performed according to U.K. Home Office regulations (Guidance on the Operation of Animals, Scientific Procedures Act 1986) and along the directives of the European Union.

### Zymosan peritonitis

The acute leukocyte migratory response was produced by i.p. injection of 1 mg of boiled zymosan A (Sigma-Aldrich) in 0.5 ml of sterile saline (29), whereas control animals were injected with an equal volume of saline. At different time points, animals were subjected to mild halothane (3%) anesthesia for collection of blood aliquots (maximum 1 ml), before sacrifice and washing of the peritoneal cavity with 3 ml of PBS supplemented with 3 mM EDTA. Then, hearts were slowly perfused with 20 ml of PBS + heparin + EDTA to remove excess blood contents in tissues, and fragments of the mesentery were collected and processed as described below. In some cases, experimental groups were treated with 0.5 mg/kg i.p. Dex (Sigma-Aldrich) or with 100 µg of peptide Ac2-26 i.p. (Ac-AMVSE FLKQAWFIENEEQEYVQTVK; obtained from the Advance Biotechnology Centre, The Charing Cross and Westminster Medical School, London, U.K.) 15 min before zymosan injection. The doses used were selected from a previous study with this model of peritonitis (30).

### Histological analyses

**Cell numbers**—Aliquots of blood (20 µl) or peritoneal lavage fluids (100 µl) were diluted 1/10 in Turk's solution (0.1% crystal violet in 3% acetic acid); total and differential counting were obtained with a Neubauer chamber using a ×40 objective and a light microscope (Zeiss). Peritoneal cells were distinguished in polymorphonuclear (PMN) and monocyte/macrophages (mono-Mφ), whereas blood cells were divided into PMN and PBMC.

**Lac-Z staining and morphological analyses**—Peritoneal and blood cells as well as tissue fragments were fixed in 4% paraformaldehyde, 0.1 M sodium phosphate buffer (pH 7.4) for 2 h at 4°C. The spatial and temporal distribution of the activated *AnxA1* gene was identified using 5-bromo-4-chloro-3-indolyl β-D-galactoside (X-Gal) staining. In the presence of β-galactosidase, this staining produces a characteristic Prussian blue color. To this end, the fixative was removed by three washes in 0.1 M phosphate buffer (pH 8), 2 mM magnesium chloride, 0.1% Triton X-100. Samples were stained overnight at 37°C with 5 mM potassium ferricyanide and 5 mM potassium ferrocyanide in rinse buffer containing 1 mg/ml β-galactosidase and 4% dimethyl-formamide. Samples were then washed in PBS at room temperature and fixed again in 4% paraformaldehyde. Finally, samples were washed in PBS, dehydrated in ethanol and embedded in LR Gold resin (London Resin). The embedded cellular or tissue samples were then cut on an ultramicrotome (Reichert Ultracut; Leica) and placed on glass slides for subsequent analysis.

**Immunohistochemistry**—LR Gold-embedded sections (1-µm thick) were incubated with 10% albumin bovine in PBS (PBSA) to block nonspecific binding. A polyclonal rabbit anti-*AnxA1* Ab (Zymed Laboratories) was added (1/200 in 1% PBSA), and slides incubated overnight at 4°C. As control for the reaction, some sections were incubated with nonimmune rabbit serum (1/200 working dilution; Sigma-Aldrich) instead of the primary Ab. After

repeated washings in 1% PBSA, a goat anti-rabbit IgG (Fc fragment-specific) Ab conjugated to 5 nm colloidal gold (1/100; British BioCell International) was added. Silver enhancing solution (British BioCell International) was used to augment gold particle staining. At the end of the reaction, sections were washed thoroughly in distilled water, counterstained with hematoxylin, and mounted in BIOMOUNT (British BioCell International). Analysis was conducted with a microscope Nikon equipped with a DXM1200 digital camera, using the software LUCIA (Laboratory Universal Computer Image Analysis; Jencons-PLS).

## Biochemical analyses

**Cytokine levels**—Aliquots of peritoneal lavage fluids were centrifuged at  $400 \times g$ , respectively, for 10 min, and tested for IL-1 $\beta$  (OpEIA; BD Biosciences) or KC (R&D Systems).

**Western blotting for AnxA1**—Blood aliquots from naive mice or after zymosan treatment, were pooled (three mice per group), and erythrocytes were sedimented in Dextran T500 (Amersham Biosciences) solution (1.25% in saline) for 30 min. The leukocyte-rich layer was harvested and incubated with a mixture of mAb targeting circulating lymphocytes and monocytes, as described (31). Briefly, mouse blood was incubated with a mixture of rat anti-mouse mAb: anti-CD2, anti-CD5, and anti-CD45R (5  $\mu\text{g/ml}$ ; BD Biosciences); anti-F4/80 (1  $\mu\text{g/ml}$ ; Serotec) and anti-CD54 (3  $\mu\text{g/ml}$ ; gift from Dr. I. Robinson (UCB-Celltech) for 30 min at 4°C, then washed and incubated with anti-rat IgG MicroBeads (20  $\mu\text{l}/10^7$  cells) for a further 15 min before running the leukocyte/MicroBead mixture through the column and collection of the neutrophil-rich population (>95% pure as determined by Gr1 staining and flow cytometry). PBMC blocked into the column were then collected by repeated washes after magnet removal. Purified PMN and PBMC were lysed with hot Laemmli sample buffer (32), and equal protein amounts (30  $\mu\text{g}$ ) electrophoresed in a 10% polyacrylamide gel in running buffer (0.3% Tris base, 1.44% glycine, 0.1% SDS in distilled water) followed by transfer of proteins onto Hybond-C extra nitrocellulose membranes in transfer buffer (0.3% Tris base, 1.44% glycine, 20% methanol in distilled water). Membranes were blocked for 1 h with 5% nonfat milk solution in TBS containing 0.1% Tween 20 followed by overnight incubation of polyclonal rabbit anti-AnxA1 (1/500; Zymed Laboratories). Equal loading was confirmed with an anti-vimentin mAb (clone VIM-13.2; Sigma-Aldrich) (data not shown). In either case, the signal was amplified with HRP-linked rat anti-rabbit secondary Ab (1/3000; Serotec) and visualized by ECL (Western blotting detection reagent; Amersham Biosciences).

## Data handling and statistical analysis

Blood and peritoneal leukocyte data are reported as mean  $\pm$  SEM of six mice per group. Quantification of cell numbers in the tissue samples was performed with a high-power objective ( $\times 40$ ) counting the cells in 100  $\mu\text{m}^2$  areas (analyzing at least 10 distinct sections per mouse). This also allowed morphological analysis of mast cell degranulation as determined by the presence of extravasated cytoplasmic granules in the connective tissue. Densitometric analysis for X-Gal staining was done according to an arbitrary scale ranging from 0 to 255 U. Statistical differences between groups were determined by ANOVA followed, if significant, by the Bonferroni test. In all cases, a probability value  $<0.05$  was taken as significant.

## Results

### Analysis of local and systemic cellular dynamics in peritonitis: impact of AnxA1 deficiency

Injection of zymosan into the mouse peritoneal cavity of WT mice produced a rapid influx of PMN, with a peak at 4 h, which then resolved up to 96 h postinjection (Fig. 1A). In

AnxA1<sup>null</sup> mice, this response was more marked with an almost ~80% increase in PMN numbers at 4 h. In these mice, the early phase was also characterized by an augmented disappearance of the M $\phi$  population (Fig. 1B). All differences were attenuated at later time points with a tendency to disappear at >24 h postzymosan. Of interest, mono-M $\phi$  values were not maintained in the AnxA1<sup>null</sup> mouse, with a significant trough (~30%) at the 48-h time point (Fig. 1B). This observation was reproducible (i.e., detected in three distinct time-course experiments, with a total number of 15 mice). Profiles of circulating cells were also altered in AnxA1<sup>null</sup> mice. In WT mice, peritoneal leukocyte trafficking was mirrored by a blood leukocytosis, at least with respect to the PMN population (Fig. 1C). Thus, absence of AnxA1 did not modify basal values for circulating cells (Fig. 1, C and D), but a failure in the postzymosan neutrophilia was observed (Fig. 1D). Alterations in PMN recruitment were associated with augmented levels of the CXC chemokine KC, with values more than doubled in AnxA1<sup>null</sup> compared with WT mice (Fig. 1E). Similarly, higher levels of the multipotent cytokine IL-1 $\beta$  could also be measured in the absence of *AnxA1* gene, with greater values than WT mice both at 4 and 24 h postzymosan (Fig. 1F).

The phenotype of the AnxA1<sup>null</sup> mouse was rescued by administering the bioactive peptide Ac2-26 (given at the dose of 100  $\mu$ g i.v. at time 0): the AnxA1 mimetic reduced peritoneal PMN recruitment (10<sup>6</sup>/mouse) in WT mice from  $3.9 \pm 0.3$  to  $2.5 \pm 0.1$  ( $n = 6$ ;  $p < 0.05$ ), and in AnxA1<sup>null</sup> mice from  $5.8 \pm 0.1$  to  $2.4 \pm 0.3$  ( $n = 6$ ;  $p < 0.05$ ). In the blood, peptide Ac2-26 reduced the number of circulating PMN in the WT mice (10<sup>6</sup>/ml) from  $16.3 \pm 0.9$  to  $5.5 \pm 0.5$  ( $n = 6$ ;  $p < 0.05$ ), as well as in AnxA1<sup>null</sup> mice (from  $9.0 \pm 1.5$  to  $6.4 \pm 0.7$ ;  $n = 6$ ;  $p < 0.05$ ). Table I reports the effect of peptide Ac2-26 on soluble proinflammatory mediators (KC and IL-1 $\beta$ ) both in WT and AnxA1<sup>null</sup> mice, as measured 4 h postzymosan.

Changes in numbers of PMN and mono-M $\phi$  cells in the lavage fluids were mirrored by changes in the mesenteric tissue, where total leukocyte influx over the complete time course (0–96 h postzymosan) was analyzed. Table II provides the cell numbers in WT and AnxA1<sup>null</sup> mice, with significant changes already seen 4 h postzymosan (~30%) with a more pronounced alteration observed at the 24-h time point. Fig. 2, A–E, show the mesenteric tissue of WT mice at the different time points, whereas Fig. 2, F–J, illustrate tissue samples collected from the AnxA1<sup>null</sup> animals. Cumulative values are in Table II, showing a higher leukocyte number in the AnxA1<sup>null</sup> mice at the 4-h time point.

This set of experiments was concluded by analysis of mast cell morphology. Mast cells (connective tissue subtype) are resident within the mesentery, in close vicinity of postcapillary venules (33) and participate actively to promote the inflammatory response to zymosan (27). Intact mast cells were found in mesenteric tissues of untreated mice. A distinct time-dependent profile of mast cell degranulation was evident upon zymosan injection. Fig. 3A illustrates an intact mast cell in WT control group, where a marked mast cell degranulation occurred within 4 h, and persisted for up to 24 h postzymosan (as determined by reduced granule staining with toluidine blue; Fig. 3, B and C). Over time, though, mast cells reacquired their morphology with integrity of their granules (Table III). In AnxA1<sup>null</sup> mice, an alteration in the degree of mast cell degranulation was evident with a more marked response being detected both at 4 and 24 h postzymosan: representative cells are shown in Fig. 3, E and F, and cumulative data in Table III.

### Local and systemic cell sources: *AnxA1* gene expression

Prompted by functional alterations detected in the local inflammatory response in absence of the *AnxA1* gene, we then monitored gene activity (using the LacZ gene reporter assay; Ref. 19) and protein expression in circulating, peritoneal, and mesenteric cells. Table IV reports the densitometric analysis for each cell type (leukocyte, endothelium, and mast cell) as determined from multiple tissue sections.

As expected (34), circulating PMN and monocytes expressed the *AnxA1* gene under basal conditions. However, the local inflammatory response provoked by zymosan produced additional time-dependent gene activation in blood cells. A representative picture, together with the semiquantitative analysis from multiple mice and leukocytes, is shown in Fig. 4A: in this condition, *AnxA1* gene activation peaked at 4 h postzymosan. To correlate these findings with protein expression, circulating PMN and PBMC were purified and their AnxA1 protein contents were determined by Western blotting analysis. Again, protein expression was easily detectable in the absence of inflammation, however, levels were clearly augmented both at 4 and 24 h postzymosan (Fig. 4B). The validity of this result was confirmed by immunohistochemistry. The image in Fig. 4B demonstrates the intracellular localization for AnxA1 immunoreactivity both in circulating PMN and PBMC at the 4-h time point.

*AnxA1* gene activity could also be monitored within the inflamed mesentery. In untreated mice, there were minimal signs of *AnxA1* gene activation in postcapillary venule endothelium (Fig. 2F). However, zymosan injection provoked intense gene activation with marked staining both in endothelial cells and adherent/extravasated PMN (Fig. 2G): extravasated leukocytes exhibited enhanced *AnxA1* gene expression in the subendothelial tissue matrix (Fig. 2, G and H, for 4 and 24 h time points). Detailed analysis of the time course for *AnxA1* gene activation indicated a long-lasting activation in the endothelium, still evident 96 h postzymosan (when other inflammatory signs had disappeared; Fig. 2J).

With respect to connective tissue mast cells, *AnxA1* gene was essentially silent in untreated mice (Fig. 3G). A modest, yet reproducible, activation of expression was detected in the early response to zymosan (Fig. 3, H and I, for 4 and 24 h time point), with staining rapidly disappearing over the time course studied (Table IV).

### Anti-inflammatory actions of Dex: impact of annexin 1 deficiency

In the second part of the study, we extended our knowledge on the functional consequences of *AnxA1* gene deficiency following treatment with the anti-inflammatory glucocorticoid Dex, and also monitored the effect of this drug on *AnxA1* gene activation in specific cell types.

Fig. 5A shows the effect of Dex on leukocyte trafficking into the peritoneal cavity: whereas the steroid inhibited PMN recruitment in WT mice, it was ineffective in *AnxA1*<sup>null</sup> mice. Of interest, the lower numbers of mono-M $\phi$  recovered from the peritoneal lavage fluid of *AnxA1*<sup>null</sup> mice were also corrected by the steroid (Fig. 5A). With respect to circulating cells, treatment of WT mice with Dex prevented the neutrophilia evident at 4 h postzymosan, restoring PMN counts to basal values (compare Fig. 5A with Fig. 1A), whereas an opposite effect was attained with respect to PBMC values (Fig. 5B): in either case, these changes were absent or much milder in *AnxA1*<sup>null</sup> mice. In WT mice, Dex markedly reduced soluble mediator generation in the peritoneal cavity by ~60%, with values of  $80 \pm 5$  pg/ml for KC and  $260 \pm 15$  for IL-1 $\beta$  ( $n = 6$ ,  $p < 0.05$ ). However, this inhibitory effect was lost in *AnxA1*<sup>null</sup> mice where higher levels of either cytokine were measured (data not shown). Similarly, mast cell morphology was also monitored finding that the steroid produced ~70% inhibition of mast cell degranulation in WT mice but was without any significant effect in *AnxA1*<sup>null</sup> mice ( $n = 6$ /group,  $p < 0.05$ ).

### Dex and *AnxA1* gene expression

A study of LacZ gene activity was then conducted to monitor the effect of Dex on *AnxA1* gene expression. In circulating cells, the steroid did not increase values for  $\beta$ -galactosidase staining above those already augmented by zymosan (see Fig. 4). In contrast, the anti-

inflammatory effect of the steroid illustrated above was associated with augmented *AnxA1* gene activation in adherent leukocytes or in cells extravasated into the subendothelial connective tissue. This augmented activation was evident both for adherent and extravasated PMN as well as adherent monocytes (Fig. 6A). Fig. 6B illustrates the intense staining observed in migrated PMN after steroid treatment. Finally, Dex failed to modify endothelial cell *AnxA1* gene activation (data not shown), whereas it produced significant increases (~40%) in *AnxA1* gene activation in the connective tissue mast cells ( $n = 6$ ;  $p < 0.05$ ).

## Discussion

It is now emerging that a complex interplay between proinflammatory and anti-inflammatory pathways occurs during ongoing inflammatory responses. This is accompanied by an increased awareness that malfunctioning or absence of endogenous tonic inhibitory mechanisms could be responsible for exacerbation of inflammation with consequent self-inflicted tissue damage (8). However, detailed analysis of when and where specific counterregulatory mechanisms operate during the time course of an inflammatory reaction has yet to be analyzed in a systematic fashion. In the present study, we have monitored expression, and function, of one of these checkpoint mechanisms, the glucocorticoid-regulated protein AnxA1: this has been possible by using AnxA1-deficient mice, bearing a construct in which the *AnxA1* gene promoter controls expression of the *LacZ* gene (19).

The zymosan peritonitis model has been used to determine the pharmacological efficacy of AnxA1 and its peptidomimetics (21, 30). The cellular events occurring during this model of resolving peritonitis, including activation of resident mast cells and macrophages (27), have also been partially studied; more recently, this model has been used to apply a multipronged lipidomic and proteomic approach to investigate pattern of delayed mediator expression (28).

Initially, we furthered our understanding of the functional consequences of AnxA1 absence by studying in detail the time course of the response to zymosan (19). AnxA1<sup>null</sup> mice exhibited increased influx of PMN as early as 4 h postzymosan, and persisting up to 24 h. Higher PMN migration was associated with exacerbation of the disappearance response of resident macrophages (35). In this model of peritonitis, rapid disappearance of macrophages occurs as early as 1–2 h (27), with a partial reappearance at 4 h postzymosan injection. This “macrophage disappearance response” is possibly linked to higher cell adhesion to serosal mucosa, perhaps consequent to coagulation system activation (36), or rapid mobilization to mesenteric lymph nodes (35) and is generally indicative of a prolonged activation status. Interestingly, AnxA1<sup>null</sup> mice exhibited reduced mono-M $\phi$  at the 48-h time point. The reason for this is unclear, however, if confirmed in other settings, it might suggest a role for AnxA1 in provoking monocyte influx, a process which is a prerequisite for restoring postinflammation homeostasis (by removing apoptotic leukocytes; Ref. 37). Finally, higher values of two specific proinflammatory mediators (KC and IL-1 $\beta$ ) were measured in the lavage fluids collected from AnxA1<sup>null</sup> mice. All the changes observed in this genotype were rescued by administering an anti-inflammatory dose of the AnxA1 mimetic peptide Ac2-26 (21), confirming their genuine link to the absence of the protein.

Analysis of the mesenteric tissue allowed further understanding of the local cellular processes. Although high numbers of adherent leukocyte adhesion were found in AnxA1<sup>null</sup> mice 4 h postzymosan, this was reflected by increased cell emigration at a later time point (24 h). Indeed, an approximate transmigrated/adherent ratio of 9 vs 4 could be calculated for AnxA1<sup>null</sup> and WT mice, respectively. This is in line with a recent study that highlighted the higher migrating and chemotactic phenotype of AnxA1<sup>null</sup> neutrophils (38). We can now

propose that these alterations within the microcirculation correlate with protein induction observed in circulating leukocytes of WT mice. The AnxA1 content of both circulating PMN and PBMC (predominantly monocytes) was augmented after zymosan injection, according to the model developed in recent years (9, 12), this acts to down-regulate PMN migration across postcapillary venules; in the AnxA1<sup>null</sup> mouse, this braking mechanism is not operative and PMN continue to extravasate even 24 h postzymosan. This is the first time that increased AnxA1 levels are reported in blood cells in an experimental model of inflammation: the mechanism is as yet unclear but possibly related to increased circulating corticosterone (M. Perretti, unpublished data). The present results clearly demonstrate increased de novo protein synthesis and, indeed, X-Gal staining confirmed intense activation of the *AnxA1* gene promoter in these circulating cells. Compared with WT mice, AnxA1<sup>null</sup> mice displayed higher mast cell degranulation at the 4-h time point, indicating the importance of this endogenous AnxA1 protein on the regulation of granules/mediators release from this cell type. Ultrastructural immunocytochemistry provided evidence that connective tissue mast cells produce and store AnxA1 in their granules and could release it under appropriate stimulation (39, 40). In this study, we could also detect a delayed activation of the *AnxA1* gene; whereas the higher degree of early mast cell degranulation could explain the higher values of KC detected in the AnxA1<sup>null</sup> mouse exudates (27), production of AnxA1 at ~96 h postzymosan might be related to a later proresolving role of this mediator on the host response. Limited functional studies have been conducted so far to address the effect of exogenously added AnxA1 on mast cell activation, though a recent analysis with rat mast cells revealed the ability of peptide Ac2-26 to inhibit OVA-evoked histamine release (41).

Analysis of the cellular events in the mesenteric tissue revealed distinct patterns of *AnxA1* gene activation indicating a strict temporal and spatial relationship for expression of this homeostatic mediator. Clear signs of *AnxA1* gene expression in postcapillary venule endothelial cells and their surrounding resident mast cells were obtained, though the most intense staining was seen in extravasated PMN and mono-M $\phi$ . The reason for such a marked induction of the *AnxA1* gene in migrated leukocytes, after the adhesion/diapedesis step at which the protein is thought to be exerting its major anti-inflammatory role (38, 42), is surprising, although corroborated by studies that have reported intense expression of PMN-derived AnxA1 in inflamed tissue (23, 43). We propose here that the marked up-regulation of AnxA1 in extravasated leukocytes subserves a proresolving and anti-inflammatory role with direct impact on PMN apoptosis (44) and their removal by the resident M $\phi$  (25), thereby promoting homeostasis. Studies on AnxA1 and leukocyte apoptosis have only been conducted in in vitro settings, but the data produced here provide strong support for the notion that AnxA1 might be an important determinant of these phenomena also in vivo.

In the final part of the study, we determined the effect of Dex. AnxA1<sup>null</sup> mice are partially resistant to the antiedema effect of Dex (19) as well as to its antimigratory properties (10); however, this is the first study to determine the functional effects associated with *AnxA1* gene regulation by this steroid. Most of the inhibitory effects of Dex were abrogated in the absence of AnxA1, confirming previous analyses conducted with immunoneutralization strategies (20, 21). Interestingly, the steroid failed to augment *AnxA1* gene-related X-Gal staining in circulating leukocytes above the levels produced by zymosan-induced inflammation, but produced a marked activation in adherent and migrated leukocytes. The ability of Dex to up-regulate the *AnxA1* gene in extravasated PMN suggests activation of signaling pathways distinct from those activated by cell adhesion to CD54 (in the vessel) or to subendothelial matrix proteins. Few studies have investigated the *AnxA1* gene promoter showing, for instance in myeloid cells, an involvement for NF-IL-6 in Dex induction of AnxA1 protein expression (45, 46), whereas a role for cAMP response elements has been established in a carcinoma cell line (47). Following the same line of reasoning, it is feasible



that the lack of Dex effect on *AnxA1* gene promoter activity in circulating PMN and PBMC indicates involvement of similar signaling pathway, perhaps activated by endogenous corticosterone released in response to the peritoneal inflammation (M. Perretti, unpublished data).

Glucocorticoids have long been known to affect mast cell maturation by interfering with stem cell factor generation and effects (48, 49). More recently, their effects on mast cell activation have also become apparent with reported ability of suppressing cytokine generations both in vitro and in vivo (50-52), an action which is likely secondary to inhibition of specific signaling pathways (53, 54). Data here presented with the *LacZ* gene reporter assay complement our previous ones (39, 40) and indicate that up-regulation of *AnxA1* might be important for bringing about the inhibitory/protective effects exerted by glucocorticoids on mast cell activation.

In this study, we delineated the role of *AnxA1* in the pathophysiology of experimental peritonitis as induced by zymosan. Absence of *AnxA1* causes an exacerbation of the inflammatory response as assessed by leukocyte influx and cytokine levels, with alterations both locally within the microcirculation and in the systemic circulation. Use of the *AnxA1*<sup>null</sup> mouse bearing a report *LacZ* gene provided clear indications for a role of the *AnxA1* gene and protein in the anti-inflammatory actions of a glucocorticoid.

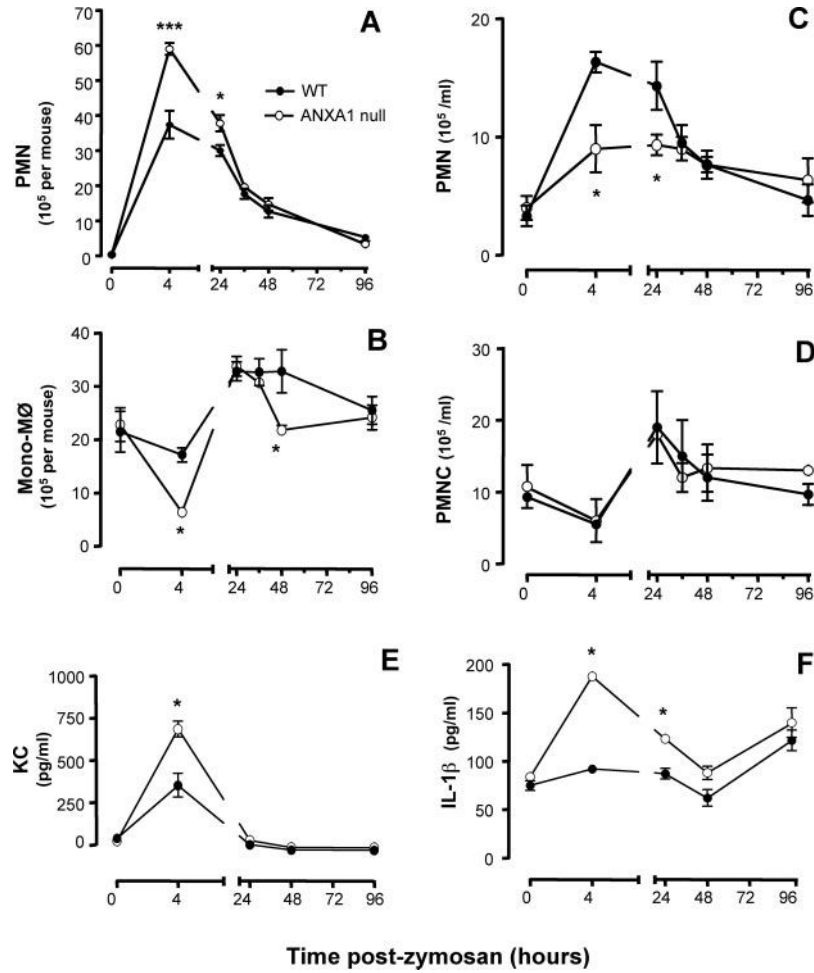
## References

1. Panés J, Granger DN. Leukocyte-endothelial cell interactions: molecular mechanisms and implications in gastrointestinal disease. *Gastroenterology*. 1998; 114:1066–1090. [PubMed: 9558298]
2. Stokes KY, Granger DN. The microcirculation: a motor for the systemic inflammatory response and large vessel disease induced by hypercholesterolemia? *J. Physiol*. 2005; 562:647–653. [PubMed: 15611017]
3. Panés J, Perry M, Granger DN. Leukocyte-endothelial cell adhesion: avenues for therapeutic intervention. *Br. J. Pharmacol*. 1999; 126:537–550. [PubMed: 10188959]
4. Nourshargh S, Marelli-Berg FM. Transmigration through venular walls: a key regulator of leukocyte phenotype and function. *Trends Immunol*. 2005; 26:157–165. [PubMed: 15745858]
5. Frangiannakis NG, Smith CW, Entman ML. The inflammatory response in myocardial infarction. *Cardiovasc Res*. 2002; 53:31–47. [PubMed: 11744011]
6. Nathan C. Points of control in inflammation. *Nature*. 2002; 420:846–852. [PubMed: 12490957]
7. Levy BD, Clish CB, Schmidt B, Gronert K, Serhan CN. Lipid mediator class switching during acute inflammation: signals in resolution. *Nat. Immunol*. 2001; 2:612–619. [PubMed: 11429545]
8. Gilroy DW, Lawrence T, Perretti M, Rossi AG. Inflammatory resolution: new opportunities for drug discovery. *Nat. Rev. Drug Discov*. 2004; 3:401–416. [PubMed: 15136788]
9. Perretti M, Flower RJ. Annexin 1 and the biology of the neutrophil. *J. Leukocyte Biol*. 2004; 75:25–29. [PubMed: 14966195]
10. Yang YH, Morand EF, Getting SJ, Paul-Clark MJ, Liu DL, Yona S, Hannon R, Buckingham JC, Perretti M, Flower RJ. Modulation of inflammation and response to dexamethasone by annexin-1 in antigen-induced arthritis. *Arthritis Rheum*. 2004; 50:976–984. [PubMed: 15022342]
11. Ernst, JD. Annexin functions in phagocytic leukocytes. In: Seaton, BA., editor. *Annexins: Molecular Structure to Cellular Function*. Austin: R.G. Landes; 1996. p. 81-96.
12. Perretti M, Croxtall JD, Wheller SK, Goulding NJ, Hannon R, Flower RJ. Mobilizing lipocortin 1 in adherent human leukocytes down-regulates their transmigration. *Nat. Med*. 1996; 22:1259–1262. [PubMed: 8898757]
13. Perretti M, Christian H, Wheller SK, Aiello I, Mugridge KG, Morris JF, Flower RJ, Goulding NJ. Annexin I is stored within gelatinase granules of human neutrophils and mobilised on the cell surface upon adhesion but not phagocytosis. *Cell. Biol. Int*. 2000; 24:163–174. [PubMed: 10772777]

14. Perretti M, Chiang N, La M, Fierro IM, Marullo S, Getting SJ, Solito E, Serhan CN. Endogenous lipid- and peptide-derived anti-inflammatory pathways generated with glucocorticoid and aspirin treatment activate the lipoxin A<sub>4</sub> receptor. *Nat. Med.* 2002; 8:1296–1302. [PubMed: 12368905]
15. Perretti M, Flower RJ. Modulation of IL-1-induced neutrophil migration by dexamethasone and lipocortin 1. *J. Immunol.* 1993; 150:992–999. [PubMed: 8423349]
16. Yang Y, Leech M, Hutchinson P, Holdsworth SR, Morand EF. Antiinflammatory effect of lipocortin 1 in experimental arthritis. *Inflammation.* 1997; 21:583–596. [PubMed: 9429906]
17. Zouki C, Ouellet S, Filep JG. The anti-inflammatory peptides, antinflammins, regulate the expression of adhesion molecules on human leukocytes and prevent neutrophil adhesion to endothelial cells. *FASEB J.* 2000; 14:572–580. [PubMed: 10698973]
18. Walther A, Riehemann K, Gerke V. A novel ligand of the formyl peptide receptor: annexin I regulates neutrophil extravasation by interacting with the FPR. *Mol. Cell.* 2000; 5:831–840. [PubMed: 10882119]
19. Hannon R, Croxtall JD, Getting SJ, Roviezzo F, Yona S, Paul-Clark MJ, Gavins FN, Perretti M, Morris JF, Buckingham JC, Flower RJ. Aberrant inflammation and resistance to glucocorticoids in annexin 1<sup>-/-</sup> mouse. *FASEB J.* 2003; 17:253–255. [PubMed: 12475898]
20. Mancuso F, Flower RJ, Perretti M. Leukocyte transmigration, but not rolling or adhesion, is selectively inhibited by dexamethasone in the hamster post-capillary venule: involvement of endogenous lipocortin 1. *J. Immunol.* 1995; 155:377–386. [PubMed: 7602112]
21. Getting SJ, Flower RJ, Perretti M. Inhibition of neutrophil and monocyte recruitment by endogenous and exogenous lipocortin 1. *Br. J. Pharmacol.* 1997; 120:1075–1082. [PubMed: 9134220]
22. Ambrose MP, Hunninghake GW. Corticosteroids increase lipocortin I in BAL fluid from normal individuals and patients with lung disease. *J. Appl. Physiol.* 1990; 68:1668–1671. [PubMed: 2140829]
23. Vergnolle N, Coméra C, Buéno L. Annexin 1 is overexpressed and specifically secreted during experimentally induced colitis in rats. *Eur. J. Biochem.* 1995; 232:603–610. [PubMed: 7556213]
24. Perretti M, Wheller SK, Flower RJ, Wahid S, Pitzalis C. Modulation of cellular annexin I in human leukocytes infiltrating DTH skin reactions. *J. Leukocyte Biol.* 1999; 65:583–589. [PubMed: 10331485]
25. Maderna P, Yona S, Perretti M, Godson C. Modulation of phagocytosis of apoptotic neutrophils by supernatant from dexamethasone-treated macrophages and annexin-derived peptide Ac2-26. *J. Immunol.* 2005; 174:3727–3733. [PubMed: 15749912]
26. Oliani SM, Paul-Clark MJ, Christian HC, Flower RJ, Perretti M. Neutrophil interaction with inflamed postcapillary venule endothelium alters annexin 1 expression. *Am. J. Pathol.* 2001; 158:603–615. [PubMed: 11159197]
27. Ajuebor MN, Das AM, Virag L, Flower RJ, Szabo C, Perretti M. Role of resident peritoneal macrophages and mast cells in chemokine production and neutrophil migration in acute inflammation: evidence for an inhibitory loop involving endogenous IL-10. *J. Immunol.* 1999; 162:1685–1691. [PubMed: 9973430]
28. Bannenberg GL, Chiang N, Ariel A, Arita M, Tjonahen E, Gotlinger KH, Hong S, Serhan CN. Molecular circuits of resolution: formation and actions of resolvins and protectins. *J. Immunol.* 2005; 174:4345–4355. [PubMed: 15778399]
29. Perretti M, Solito E, Parente L. Evidence that endogenous interleukin-1 is involved in leukocyte migration in acute experimental inflammation in rats and mice. *Agents Actions.* 1992; 35:71–78. [PubMed: 1509980]
30. Perretti M, Ahluwalia A, Harris JG, Goulding NJ, Flower RJ. Lipocortin-1 fragments inhibit neutrophil accumulation and neutrophil-dependent edema in the mouse: a qualitative comparison with an anti-CD11b monoclonal antibody. *J. Immunol.* 1993; 151:4306–4314. [PubMed: 8409403]
31. Cotter MJ, Norman KE, Hellewell PG, Ridger VC. A novel method for isolation of neutrophils from murine blood using negative immunomagnetic separation. *Am. J. Pathol.* 2001; 159:473–481. [PubMed: 11485906]
32. Laemmli UK. Cleavage of structural proteins during the assembly of the head of bacteriophage T4. *Nature.* 1970; 227:680–685. [PubMed: 5432063]

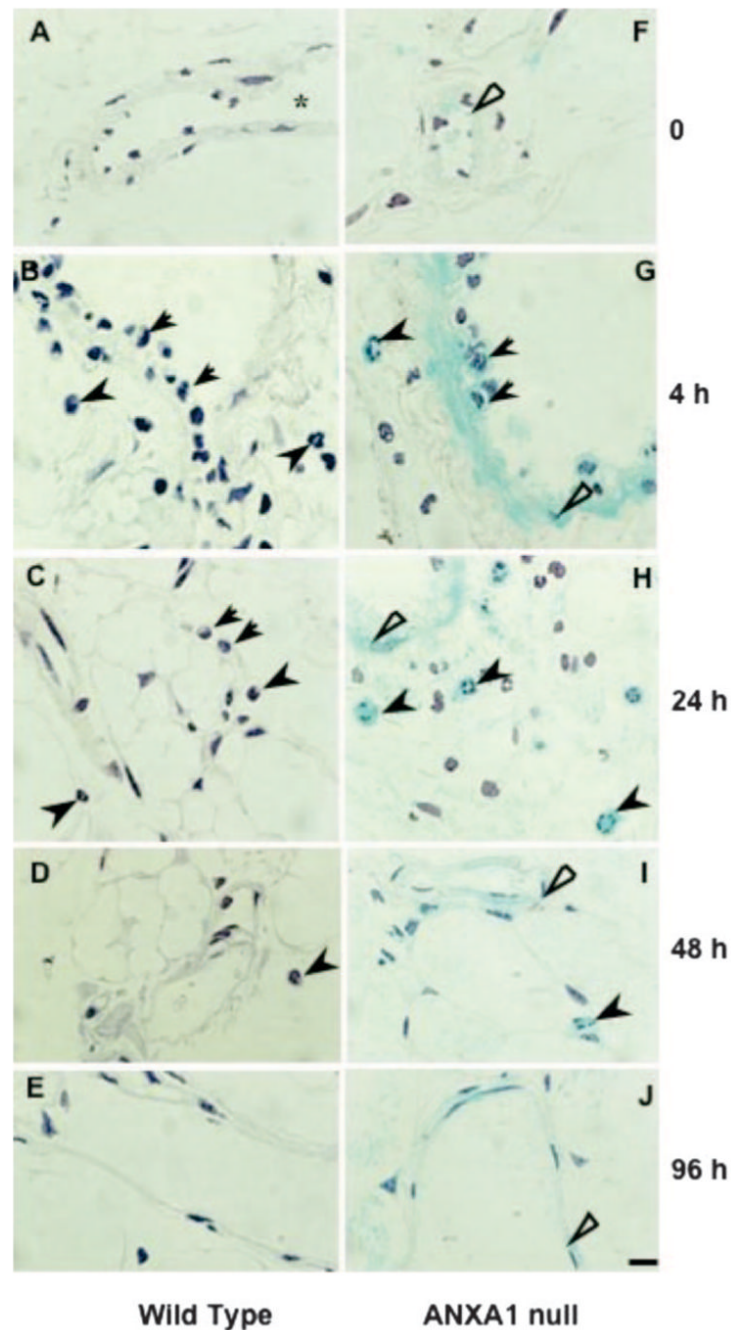
33. Kubes P, Granger DN. Leukocyte-endothelial cell interactions evoked by mast cells. *Cardiovasc. Res.* 1996; 32:699–708. [PubMed: 8915188]
34. Damazo AS, Yona S, D'Acquisto F, Flower RJ, Oliani SM, Perretti M. Critical protective role for annexin 1 gene expression in the endotoxemic murine microcirculation. *Am. J. Pathol.* 2005; 166:1607–1617. [PubMed: 15920146]
35. Barth MW, Hendrzak JA, Melnicoff MJ, Morahan PS. Review of the macrophage disappearance reaction. *J. Leukocyte Biol.* 1995; 57:361–367. [PubMed: 7884305]
36. Serra MF, Diaz BL, Barreto EO, Cordeiro RS, Nazare Meirelles MN, Williams TJ, Martins MA, Silva PM. Mechanism underlying acute resident leukocyte disappearance induced by immunological and non-immunological stimuli in rats: evidence for a role for the coagulation system. *Inflamm. Res.* 2000; 49:708–713. [PubMed: 11211922]
37. Gilroy DW, Colville-Nash PR, McMaster S, Sawatzky DA, Willoughby DA, Lawrence T. Inducible cyclooxygenase-derived 15-deoxy( $\delta$ )12–14PGJ2 brings about acute inflammatory resolution in rat pleurisy by inducing neutrophil and macrophage apoptosis. *FASEB J.* 2003; 17:2269–2271. [PubMed: 14563690]
38. Chatterjee BE, Yona S, Rosignoli G, Young RE, Nourshargh S, Flower RJ, Perretti M. Annexin 1 deficient neutrophils exhibit enhanced transmigration in vivo and increased responsiveness in vitro. *J. Leukocyte Biol.* 2005; 78:639–646. [PubMed: 16000391]
39. Oliani SM, Christian HC, Manston J, Flower RJ, Perretti M. An immunocytochemical and in situ hybridization analysis of annexin 1 expression in rat mast cells: modulation by inflammation and dexamethasone. *Lab. Invest.* 2000; 80:1429–1438. [PubMed: 11005211]
40. Damazo A, Paul-Clark MJ, Straus AH, Takahashi HK, Perretti M, Oliani SM. Analysis of annexin 1 expression in rat trachea: study of the mast cell heterogeneity. *Annexins.* 2004; 1:12–18.
41. Bandeira-Melo C, Bonavita AG, Diaz BL, e Silva PMR, Carvalho VF, Jose PJ, Flower RJ, Perretti M, Martins MA. A novel effect for annexin 1-derived peptide ac2-26: reduction of allergic inflammation in the rat. *J. Pharmacol. Exp. Ther.* 2005; 313:1416–1422. [PubMed: 15784654]
42. Gavins FN, Yona S, Kamal AM, Flower RJ, Perretti M. Leukocyte antiadhesive actions of annexin 1: ALXR- and FPR-related anti-inflammatory mechanisms. *Blood.* 2003; 101:4140–4147. [PubMed: 12560218]
43. D'Amico M, Di Filippo C, La M, Solito E, McLean PG, Flower RJ, Oliani SM, Perretti M. Lipocortin 1 reduces myocardial ischaemia-reperfusion injury by affecting local leukocyte recruitment. *FASEB J.* 2000; 14:1867–1869. [PubMed: 11023969]
44. Solito E, Kamal AM, Russo-Marie F, Buckingham JC, Marullo S, Perretti M. A novel calcium-dependent pro-apoptotic effect of annexin 1 on human neutrophils. *FASEB J.* 2003; 17:1544–1546. [PubMed: 12824302]
45. Solito E, de Coupade C, Parente L, Flower RJ, Russo-Marie F. IL-6 stimulates annexin 1 expression and translocation and suggests a new biological role as class II acute phase protein. *Cytokine.* 1998; 10:514–521. [PubMed: 9702415]
46. Solito E, de Coupade C, Parente L, Russo-Marie F. Human annexin 1 is highly expressed during differentiation of the epithelial cell line A549: involvement of nuclear factor interleukin 6 in phorbol ester induction of annexin 1. *Cell Growth Differ.* 1998; 9:327–336. [PubMed: 9563852]
47. Antonicelli F, De Coupade C, Russo-Marie F, Le Garrec Y. CREB is involved in mouse annexin A1 regulation by cAMP and glucocorticoids. *Eur. J. Biochem.* 2001; 268:62–69. [PubMed: 11121103]
48. Jeong HJ, Na HJ, Hong SH, Kim HM. Inhibition of the stem cell factor-induced migration of mast cells by dexamethasone. *Endocrinology.* 2003; 144:4080–4086. [PubMed: 12933682]
49. Galli SJ, Kalesnikoff J, Grimbaldeston MA, Piliponsky AM, Williams CM, Tsai M. Mast cells as “tunable” effector and immunoregulatory cells: recent advances. *Annu. Rev. Immunol.* 2005; 23:749–786. [PubMed: 15771585]
50. Wershil BK, Furuta GT, Lavigne JA, Choudhury AR, Wang Z-S, Galli SJ. Dexamethasone or cyclosporin A suppress mast cell-leukocyte cytokine cascade: multiple mechanisms of inhibition of IgE- and mast cell-dependent cutaneous inflammation in the mouse. *J. Immunol.* 1995; 154:1391–1398. [PubMed: 7822805]

51. Schramm R, Schaefer T, Menger MD, Thorlacius H. Acute mast cell-dependent neutrophil recruitment in the skin is mediated by KC and LFA-1: inhibitory mechanisms of dexamethasone. *J. Leukocyte Biol.* 2002; 72:1122–1132. [PubMed: 12488493]
52. Tailor A, Tomlinson A, Salas A, Panés J, Granger DN, Flower RJ, Perretti M. Dexamethasone inhibition of leucocyte adhesion to rat mesenteric postcapillary venules: role of intercellular adhesion molecule 1 and KC. *Gut.* 1999; 45:705–712. [PubMed: 10517906]
53. Hiragun T, Peng Z, Beaven MA. Dexamethasone up-regulates the inhibitory adaptor protein Dok-1 and suppresses downstream activation of the mitogen-activated protein kinase pathway in antigen-stimulated RBL-2H3 mast cells. *Mol. Pharmacol.* 2005; 67:598–603. [PubMed: 15608142]
54. Cissel DS, Beaven MA. Disruption of Raf-1/heat shock protein 90 complex and Raf signaling by dexamethasone in mast cells. *J. Biol. Chem.* 2000; 275:7066–7070. [PubMed: 10702272]



**FIGURE 1.**

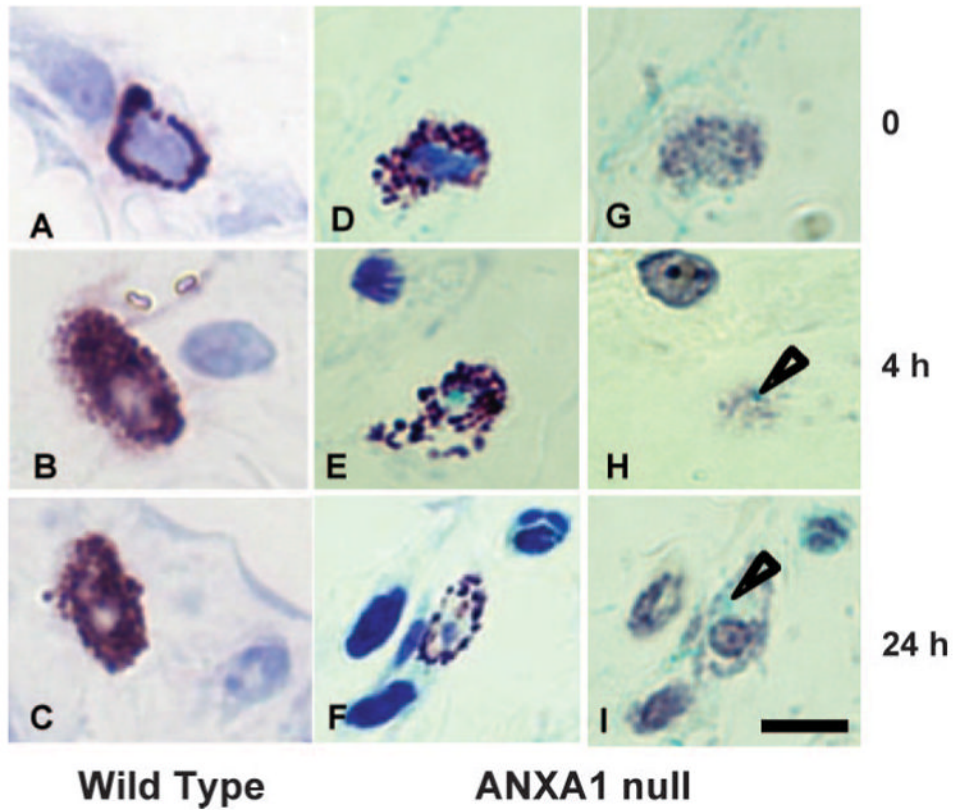
Time course of leukocyte influx in the peritoneal cavity, leukocytosis in the blood and inflammatory cytokine production. WT and AnxA1<sup>null</sup> mice received 1 mg of zymosan i.p. at time 0. At different time points, peritoneal cavities were washed for PMN and mono-Mφ quantification (A and B); blood aliquots were also collected for measuring PMN and PBMC (PBMC; C and D). The concentrations of KC (E) and IL-1β (F) were determined in the peritoneal lavage washes. Data are mean ± SEM from two separate experiments with five mice each. 0, *p* < 0.05 vs corresponding WT value.



**FIGURE 2.**

Analysis of cell migration in the mesenteric tissue. WT and *AnxA1*<sup>null</sup> mice received 1 mg of zymosan at time 0 and mesenteries were harvested at different time points. Samples were processed for the X-Gal staining and hematoxylin counterstaining as described in *Materials and Methods*. *A–E*, WT mice: *A*, control mesentery showing absence of adherent leukocytes in the vessels (\*). *B–D*, Some leukocytes are observed intravascularly (arrows) and transmigrated to the tissue (arrowheads) 4, 24, or 48 h postzymosan. They are no longer present at 96 h postzymosan (*E*). *F–J*, *AnxA1*<sup>null</sup> mice: *F*, in control tissue, a light blue stain is observed on the endothelial cell layer (open arrow). *G–I*, LacZ-positive cells were observed in the mesenteric tissue 4, 24, and 48 h postzymosan: intravascular leukocytes

(arrows) are in close contact with endothelial cells (open arrows) and transmigrated leukocytes (arrowhead) are located in the connective tissue. *J*, During the resolution phase of inflammation, only mesenteric endothelial cells (open arrow) display LacZ positive staining. Bars, 10  $\mu\text{m}$ .

**FIGURE 3.**

Mast cell degranulation and *AnxA1* gene activation in mesentery. *A–C*, WT and (*D–I*) *AnxA1*<sup>null</sup> mice received 1 mg of zymosan at time 0 and mesenteries were harvested at different time points. For morphological analysis, the mesentery was stained with toluidine blue (*A–F*). *A* and *D*, Control mesentery showing intact mast cells. Degranulated mast cells in WT and *AnxA1*<sup>null</sup> mice are seen both at 4h (*B* and *E*) and 24 h (*C* and *F*) postzymosan. A more intense degranulation process was observed in the mast cells from *AnxA1*<sup>null</sup> mice. For LacZ investigation, samples were processed for X-Gal staining and counterstained with hematoxylin as described in *Materials and Methods* (*G–I*). *G*, Mast cell *AnxA1*<sup>null</sup> mice in control group was negative for LacZ. *H* and *I*, During the inflammatory reaction, degranulated mast cells were LacZ positive (open arrows). Bars, 10  $\mu$ m.



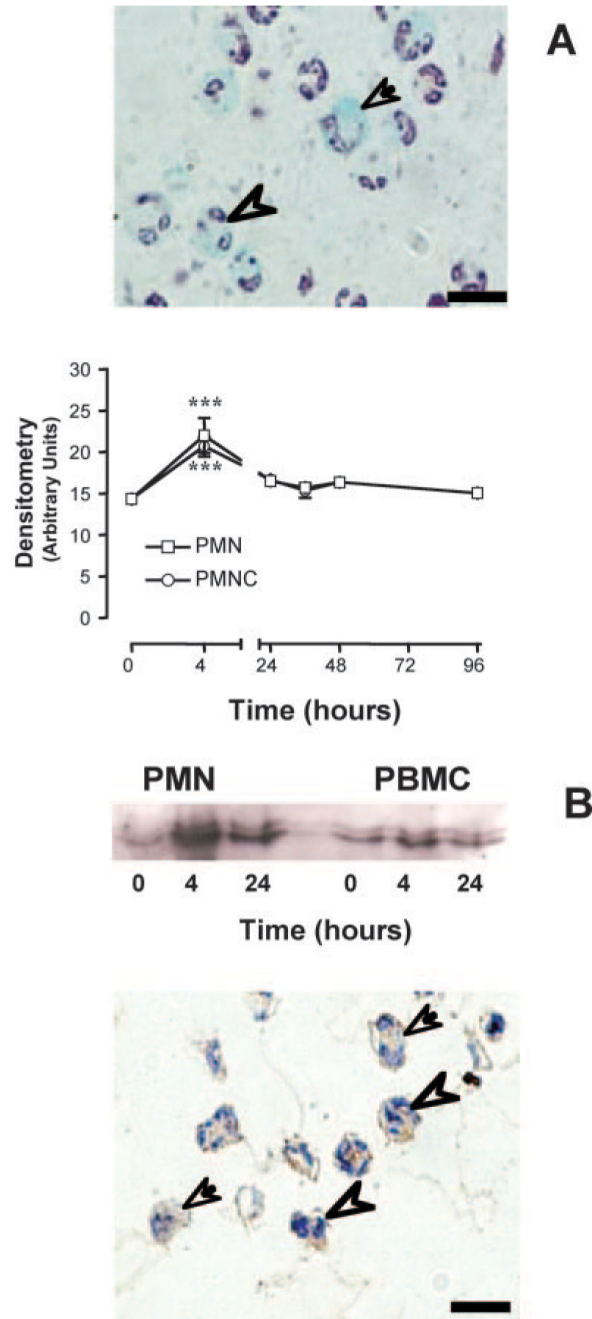


**FIGURE 4.**

Analysis of LacZ gene and AnxA1 protein expression in peripheral blood PMN and PBMC cells. Mice received 1 mg i.p. injection of zymosan at time 0 and the blood was collected at different time points. *A*, LacZ-positive PMN (arrowhead) and monocytes (arrow) were monitored for semiquantitative analysis of cell-associated LacZ. Data are mean  $\pm$  SEM of five mice per group. \*,  $p < 0.05$  vs corresponding time 0 value. *B*, AnxA1 protein content was analyzed by Western blotting. Immunohistochemistry was performed to visualize the protein in neutrophils (arrowheads) and monocytes (arrows). With both protocols, a specific rabbit polyclonal anti-annexin 1 serum was used. Hematoxylin stain. Bars, 10  $\mu$ m.

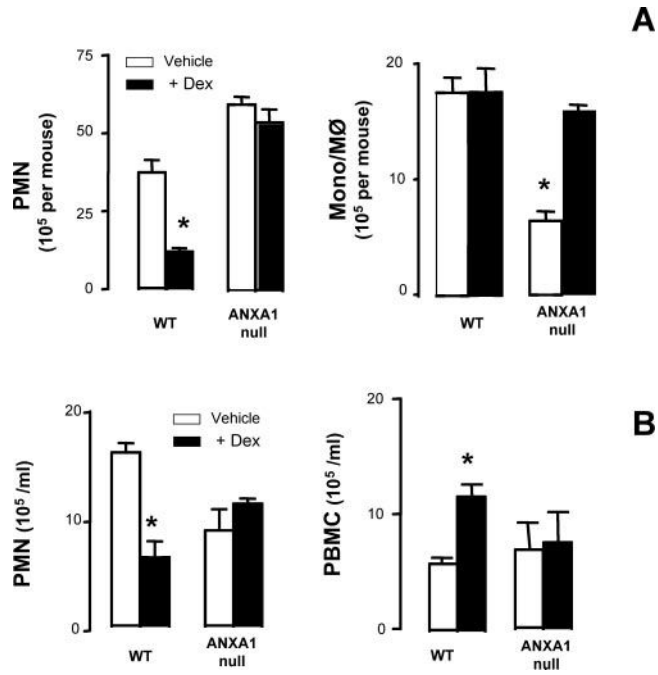


**FIGURE 5.** Leukocyte in the blood and influx into the peritoneal cavity after Dex treatment. WT and AnxA1<sup>null</sup> mice received 1 mg of zymosan i.p. at time 0. Some animals were pretreated with Dex i.p. (0.5 mg/kg) followed by zymosan administration. At the 4-h time point, peritoneal wash (A) was collected for quantification of PMN and mono-Mφ. The same procedure was used for blood aliquots (B) monitoring PMN and PBMC. Data are mean ± SEM from two different experiments with five mice each. \*, *p* < 0.05 vs corresponding control group value.

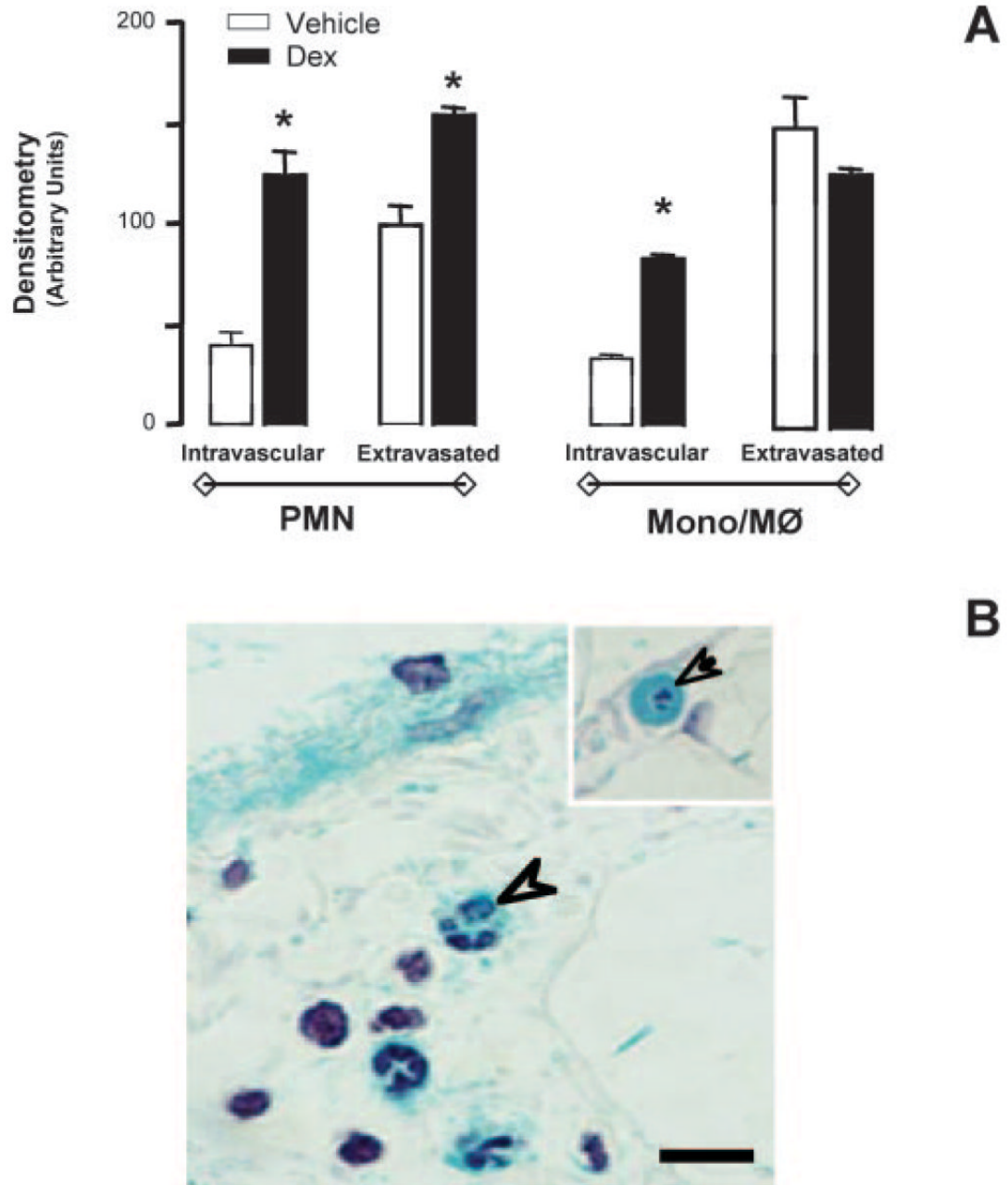


**FIGURE 6.**

*AnxA1* gene expression after 4 h zymosan stimulation in mice pretreated with Dex. *A*, Semiquantitative LacZ densitometric analysis was performed on mesenteric PMN and mono-Mφ cells 4 h postzymosan: the effect of a pretreatment with 0.5 mg/kg i.p. Dex was determined. *B*, The neutrophils (arrowhead) and monocytes (arrow) showed intense LacZ positivity after Dex stimulation. *Inset*, An intravascular monocyte in the Dex-treated group. Bars, 10 μm.

**Table I**Effect of peptide Ac2–26 on soluble mediator release<sup>a</sup>

Genotype	Treatment	KC (pg/ml)	IL-1 $\beta$ (pg/ml)
Wild type	Vehicle	225 $\pm$ 55	810 $\pm$ 25
Wild type	Peptide Ac2–26	100 $\pm$ 30 <sup>b</sup>	475 $\pm$ 15 <sup>b</sup>
AnxA1 <sup>null</sup>	Vehicle	470 $\pm$ 60 <sup>c</sup>	1210 $\pm$ 40 <sup>c</sup>
AnxA1 <sup>null</sup>	Peptide Ac2–26	200 $\pm$ 60 <sup>b</sup>	510 $\pm$ 20 <sup>b</sup>

<sup>a</sup>Mice received 100  $\mu$ g of peptide Ac2–26 i.v. or vehicle immediately before the i.p. injection of 1 mg of zymosan. Peritoneal lavage fluids were collected 4 h later and analysed for KC and IL-1 $\beta$  levels. Data are mean  $\pm$  SEM of 6 mice/group.

<sup>b</sup> $p$  < 0.05 vs respective vehicle group.

<sup>c</sup> $p$  < 0.05 vs corresponding group in the different genotype (Bonferroni test).

**Table II**Semi-quantitative analysis of leukocyte trafficking in the mouse mesentery<sup>a</sup>

Time (h)	WT		AnxA1 <sup>null</sup>	
	Intravascular	Transmigrated	Intravascular	Transmigrated
4	4.2 ± 0.6	2.0 ± 0.5	6.5 ± 0.5 <sup>b</sup>	3.5 ± 0.5
24	0.6 ± 0.4	2.3 ± 0.3	1.0 ± 0.2 <sup>b</sup>	8.6 ± 0.6 <sup>b</sup>
36	0	0.2 ± 0.1	0	0.1 ± 0.2
48	0	0.3 ± 0.2	0	0.3 ± 0.2
96	0	0	0	0

<sup>a</sup>WT and AnxA1<sup>null</sup> mice were treated with zymosan (1 mg i.p.) at time 0 and mesenteries collected at the reported time points. Histological preparation was done as described in *Materials and Methods*. Values (number of cells per mm<sup>2</sup>) are expressed as mean ± SEM of 10 tissue sections analyzed from 5 mice/group.

<sup>b</sup>*p* < 0.05 vs corresponding group in the different genotype (Bonferroni test).

**Table III**

Semiquantitative analysis of mast cell morphology in the mouse mesentery.<sup>a</sup>

Time (h)	WT		AnxA1 <sup>null</sup> mouse	
	Intact	% Degranulated	Intact	% Degranulated
0	14 ± 5	0	12 ± 4	0
4	6 ± 4	8 ± 7	2 ± 3	14 ± 5
24	7 ± 3	6 ± 7	4 ± 3	8 ± 3
36	12 ± 5	0	13 ± 2	0
48	15 ± 2	0	16 ± 6	0
96	13 ± 4	0	11 ± 5	0

<sup>a</sup>WT and AnxA1<sup>null</sup> mice were treated with zymosan (1 mg i.p.) at time 0 and mesenteries collected at the reported time points. Histological preparation was performed as described in *Materials and Methods*. Values (number of cells per 100 mm<sup>2</sup>) are expressed as mean ± SEM of 10 tissue sections analyzed from 5 mice/group.

<sup>b</sup> *p* < 0.05 vs correspondent group in the different genotype (Bonferroni test).

Table IV

Densitometric analysis of LacZ gene expression in specific mesenteric cells<sup>a</sup>

Time (h)	PMN			Mono-Mφ			Mast Cell
	Intravascular	Transmigrated	Intravascular	Transmigrated	Endothelial Cell		
0	N/A	N/A	N/A	N/A	20 ± 2	0	
4	44 ± 5	94 ± 4 <sup>b</sup>	33 ± 3	79 ± 4 <sup>b</sup>	52 ± 4 <sup>c</sup>	48 ± 4 <sup>c</sup>	
24	32 ± 2	63 ± 5 <sup>b</sup>	30 ± 3	37 ± 4	21 ± 3	30 ± 2 <sup>c</sup>	
36	N/A	94 ± 4	N/A	75 ± 5	28 ± 3	0	
48	N/A	97 ± 23	N/A	65 ± 5	25 ± 2	0	
96	N/A	N/A	N/A	N/A	18 ± 4	60 ± 5 <sup>c</sup>	

<sup>a</sup> AnnA1 null mice were treated with zymosan (1 mg i.p.) at time 0 and mesenteries collected at the reported time points. Histological preparation was done as described in *Materials and Methods*. Values (arbitrary units) are expressed as mean ± SEM of 10 tissue sections analyzed from 5 mice/group.

<sup>b</sup>  $p < 0.05$  vs correspondent intravascular values; (Bonferroni test), N/A, cells not available.

<sup>c</sup>  $p < 0.05$  vs corresponding time 0 value.